Determining appropriate imaging parameters for kilovoltage intrafraction monitoring: an experimental phantom study

D Wallace[1], J A Ng[1,2], P J Keall[2], R T O'Brien[2], P R Poulsen[4], P Juneja[1,3] and J T Booth[1,3]

[1] School of Physics, University of Sydney, NSW 2006, Australia
[2] School of Medicine, University of Sydney, NSW 2006, Australia
[3] Northern Sydney Cancer Centre, Royal North Shore Hospital, NSW 2065, Australia
[4] Department of Oncology, Aarhus University Hospital, Nørrebrogade 44, 8000 Aarhus C, Denmark

Corresponding Author: Jeremy Booth Jeremy.booth@health.nsw.gov.au

Acknowledgments

The authors acknowledge funding from the Australian National Health and Medical Research Council and Cancer Australia. Varian Medical Systems is acknowledged for providing the use of the iTools Capture software and associated hardware to allow image streaming from the OBI to the KIM software.

Abstract

Kilovoltage intrafraction monitoring (KIM) utilises the kV imager during treatment for real-time tracking of prostate fiducial markers. However, its effectiveness relies on sufficient image quality for the fiducial tracking task. To guide the performance characterisation of KIM under different clinically relevant conditions, the effect of different kV parameters and patient size on image quality, and quantification of MV scatter from the patient to the kV detector panel were investigated in this study.

Image quality was determined for a range of kV acquisition frame rates, kV exposure, MV dose rates and patient sizes. Two methods were used to determine image quality; the ratio of kV signal through the patient to the MV scatter from the patient incident on the kilovoltage detector, and the signal-to-noise ratio (SNR). The effect of patient size and frame rate on MV scatter was evaluated in a homogeneous CIRS pelvis phantom and marker segmentation was determined utilising the Rando phantom with embedded markers.

MV scatter incident on the detector was shown to be dependent on patient thickness and frame rate. The segmentation code was shown to be successful for all frame rates above 3 Hz for the Rando phantom corresponding to a kV to MV ratio of 0.16 and an SNR of 1.67. For a maximum patient dimension less than 36.4 cm the conservative kV parameters of 5 Hz at 1 mAs can be used to reduce dose while retaining image quality, where the current baseline kV parameters of 10 Hz at 1 mAs is shown to be adequate for marker segmentation up to a patient dimension of 40 cm.

In conclusion, the MV scatter component of image quality noise for KIM has been quantified. For most prostate patients, use of KIM with 10 Hz imaging at 1 mAs is adequate however image quality can be maintained and imaging dose reduced by altering existing acquisition parameters.

1. **Introduction**

Prostate SBRT benefits from continuous monitoring of target when gating or delivery adaptation is applied. Continuous monitoring with a 2 mm gating threshold is shown to prevent 10% geographic miss rate and real-time adaptation is shown to ensure target coverage within 1% (Sandler et al 2010, Colvill et al 2014, Lovelock et al 2015) Kilovoltage Intrafraction Monitoring (KIM) using kV images acquired during radiotherapy delivery has been demonstrated to be an accurate and potentially widely applicable technique for tracking intra-fraction tumour motion (Poulsen et al 2008, Ng et al 2012). Application of KIM will always deliver some imaging dose additional to the prescription (Crocker et al 2012, Ng et al 2012). KIM relies on adequate kV image quality to segment fiducial markers, but during treatment the MV scatter from the patient to the kV detector panel adds residual noise. There are many factors that will affect the image quality and segmentation success rate including kV source parameters, kV detector parameters, MV treatment beam parameters and patient-related factors. (Seibert 2004, van Herk et al 2011, Ling et al 2011b) This study concentrates on utilisation of traditional x-ray metrics, no post-processing methods were examined.

The patient size will directly affect the transmission and scatter of radiation to the kV detector panel so for broad application of KIM across a population the kV source, kV panel and treatment parameters will need to be adjusted to balance image quality and imaging dose. Following ALARA, patient specific settings should be used to minimise imaging dose. Crocker et al (Crocker et al 2012) have shown that a kV aperture of $6 \times 6\ \mathrm{cm}^2$ encompasses the prostate plus a tracking margin while retaining low imaging dose, and the highest available kVp can be used to increase penetration of the kV beam through the patient. Extending the kV source-detector-distance (SDD) (e.g. to 180 cm) reduces the MV scatter on the kV imaging panel. (Luo et al 2008) Adamson and Wu (Adamson and Wu 2009) showed that increasing the treatment field size increases the MV scatter detected on the kV panel.

The purpose of this study is to evaluate parameters affecting KIM image quality across a range of patient (phantom) dimensions to strengthen the parameter set used for patient treatment. We determine a set of beam properties to achieve successful segmentation with minimal dose and quantitate the MV scatter component of image noise for various kV source settings and kV detector settings. A model is developed to extend the application to patient specific settings.

2. **Materials and methods**

Measurements were performed on a Trilogy linac (Varian Medical Systems, Palo Alto) with the On Board Imager (OBI) flat panel detector AS1000. In this study, the sensitivity to different kV, MV and patient size parameters are assessed to determine their effect on fiducial marker segmentation success rates for KIM during treatment. Based on previous work from Ng et al (2012), we define a baseline set of kV parameters where; the kV source is set to 125 kVp, 1mAs with a field size of 6x6cm2 and no additional filtration of the x-rays by a bowtie filter. The kV detector is referenced to 10 Hz and is positioned at 180 SDD. The MV dose rate is defined at 200 MU min^{-1} and the CIRS™ (CIRS Inc., Norfolk, VA) phantom geometry is defined as our baseline geometry. Throughout this study four parameters are modified and assessed including kV exposure, kV frame rate, patient size and MV dose rate. Crocker et al (Crocker et al 2012) determined that the overall imaging doses for KIM were 0.1–0.25% of the prescribed dose with 120 kV/1.04 mAs for 80 Gy standard fractionation IMRT/VMAT and a 38Gy SBRT treatment. This imaging dose will increase to 1–2.5% when the frame rate is increased to 10 Hz.

To determine the signal to noise ratio (SNR) and segmentation rate two different types of phantoms were used; the homogeneous CIRS™ IMRT freepoint phantom (Model 002H9K, CIRS Inc, Norfolk, VA) and the Rando pelvis phantom (Model RAN100, The Phantom Laboratory, Greenwich, NY).

2.1. Experimental evaluation of image quality

2.1.1. Segmentation.

We utilised the segmentation code of Fledelius et al (Poulsen et al 2009, Fledelius et al 2011) previously used for the KIM clinical observation study (Ng et al 2012) and currently used in a prospective clinical trial (NCT01742403). Three cylindrical gold fiducial markers (1 mm diameter × 3 mm length, Civco) were embedded into the Rando pelvis. A single VMAT plan was generated using a CT scan of the RANDO pelvis phantom and this treatment plan was delivered to both Rando pelvis or CIRS phantom as required. Contouring of the prostate volume was completed to contain the three fiducial markers and a treatment plan generated to deliver 2Gy per fraction using Eclipse (Varian Medical Systems, Palo Alto).

The frame rate for kilovoltage imaging is applied on Varian linacs as a collection time separate to the kilovoltage beam pulse and pulse rate, therefore varying the kV frame rate will vary the time for MV scatter collection with constant kilovoltage signal. Frame rate is utilised as the determinant for image quality and segmentation success. We vary frame rate over the range one to fifteen Hz with all other baseline settings maintained. The image quality is determined for each of these settings.

2.1.2. Image quality determination (kV to MV ratio and SNR at the detector).

We utilise two metrics to quantify image quality; the raw ratio of kV to MV signal (pixel value) and the SNR defined by Rose (Rose 1948). The homogeneous CIRS phantom is used to measure the SNR to avoid heterogeneities in the images used for image quality calculations.

We determine the raw kV to MV signal as the ratio of kV transmission through the object ('signal') to the patient MV scatter at the kV detector panel ('noise'). The kV signal is measured as the mean pixel value in a square region of interest ($6 \times 6\ cm^2$) to represent the size of the primary kV signal on the detector, 40 frames were acquired on average. The MV patient scatter at the kV detector plane is measured in a similar way using a very low current kV beam concurrently to 'activate' the read-out of the kV detector panel. The chosen low current kV beam is 40 kVp, 0.02 mAs and was evaluated alone to give only background noise at the image panel. All analysis was conducted with in-house software using MATLAB.

This method assumes knowledge of the statistical noise and that a direct measurement of the statistical noise has been made. With knowledge of the signal and noise the division of these two values will give the basic description of image quality defined in equation (1).

$$kV\ to\ MV\ Ratio = \frac{kV\ signal}{MV\ scatter\ on\ kVD} \quad (1)$$

The second method used to describe the image quality of a single image is the SNR. The SNR considers the detectability of a flat-topped, sharp-edged signal of area, A, in a uniform background which was first defined by Rose et al (Rose 1948) and revisited in Burgess et al (Rose 1948, Burgess 1999). Using the corresponding mean photon densities, $< \Delta Ns >$ extra photons per unit area for the signal, and $< Nb >$ expected photons per unit area for the background, a signal contrast, $C = \frac{< \Delta Ns >}{< Nb >}$, Rose defined SNR with the equation (2) (Rose 1948).

$$SNR = \frac{mean\ signal}{\sigma_{Nb}} = \frac{<\Delta N_s>}{\sigma_{Nb}} \quad (2)$$

2.1.3. Effect of kV exposure and frame rate on image quality.

Measurements of the SNR require an image to be acquired with both the kV and MV beams on. Calculation of the SNR was implemented in user-written code in MATLAB. Evaluation of exposure and frame rate on image quality is measured in the CIRS phantom. The CIRS phantom is positioned on the treatment couch at the mechanical isocentre and three sets of images; kV only, kV + MV and MV only are acquired for each alteration of the kV parameters. Four exposure sets are used; 0.5 mAs, 1 mAs, 1.5 mAs and 2 mAs for four frame rates of 1 Hz, 5 Hz, 10 Hz and 15 Hz at the AP kV projection angle. The uncertainty in the measurements of the effect of imaging parameters, frame rate and kV exposure, on the image quality was quantified using coefficient of variation. Coefficient of variation was determined for all pairwise combinations of frame rates and kV exposures, and for each of the image quality metric, SNR and kV to MV ratio. Figure 1 shows the kV projection angle AP this was chosen to represent the maximum MV scatter and respectively the maximum kV signals that could occur during gantry rotation for the CIRS phantom. The AP kV projection will have a higher kV signal due to attenuation of the kV beam. The MLC files were extracted from the DICOM patient export files using an in-house MATLAB code that exports the MLC leaf positions at each control point throughout the plan. The MLC leaf positions at each control point are then extracted using Shaper (v7.0, 2007).

2.1.4. Effect of patient size on image quality.

The effect of patient size on image quality was measured by using water-equivalent material to increase the patient size (as shown in figure 1). This water-equivalent material was used to imitate six discrete patient sizes on the CIRS phantom. The patient dimensions were determined from the Australian Bureau of Statistics (ABS) who measured the waist circumference size for 15 600 households from 2011–2013 for a set of age groups and determined their average circumference size (Morris et al 2012). The average size of 99.7 cm reported by the ABS is similar to data from the USA of 100.8 cm, and UK of 97.7 cm (Maria Aresu).

The measurement of image quality for various patient sizes was performed using the baseline kV settings for each discrete patient size and using the static MLC files at respective kV projection angles with a dose rate of 200 MU s^{-1}. Images were acquired at three different gantry angles i.e. AP, lateral and PA kV projection angles. The AP and PA projection angles shared the same aperture shape. At each angle three sets of images were acquired including kV only, MV only and kV + MV for six different patient dimensions i.e. 2.5 cm, 7.5 cm, 10 cm, 15 cm and 20 cm of water-equivalent material added to the anterior surface of the CIRS phantom. The CIRS phantom is 10cm from centre to top and 15 cm from centre to side. The patient dimensions used cover the range 80 cm to 100 cm circumference.

2.1.5. Effect of MV dose rate on image quality.

The dose rate of 200 MU min^{-1} was chosen as the reference dose rate for the static gantry angles since it represents the dose rate delivered at the respective gantry angle during pelvic dual arc VMAT delivery at our Institution. To evaluate the effect of dose rate of MV scatter three different dose rates were used 200 MU min^{-1}, 400 MU min^{-1} and 600 MU min^{-1}, these dose rates were delivered using the static MLC field sizes for each kV projection angle.

2.2. Theoretical evaluation of image quality using measured and literature values

2.2.1. Modelling of MV Signal and kV Signal onto the kV Detector.

Using the theoretical definition of scatter defined in the paper by Spies et al (2000) the MV scatter incident on the kV detector can be estimated for varying patient sizes. The MV scatter is separated into two parts, the scatter of the primary beam and MV scatter at 90° from the isocentre to the detector; the equations (4) and (5) in the appendix are used to determine the MV scatter at the detector. The linear attenuation co-efficient for the primary beam, the scattered beam and a constant is determined using the data.

The kV attenuation is modelled using the measured data in this study and equation (6) in the appendix. This equation is based on the attenuation of the kV beam as it travels through varying thicknesses where the linear attenuation co-efficient and constant is determined. The above method was used to model for the effects of patient size on image quality where the kV signal and the MV scatter with patient size were evaluated.

3. **Results**

3.1. Segmentation

A frame rate of 3 Hz was observed to be the lowest frame rate for segmentation of the fiducial markers in the Rando phantom using the code by Fledelius et al (Poulsen et al 2009, Fledelius et al 2011). Table 1 shows segmentation success rate against image quality as controlled by altering the frame rate for the reference kV parameters, reference geometry and MV beam settings defined previously.

3.2. Image quality determination (kV to MV ratio and SNR at the detector)

A quasi-linear trend in the SNR and kV to MV ratio with frame rate and kV exposure is shown in figure 2. The limitation in determining image quality using the SNR equation is evident due to the sensitivity of the SNR equation to differences in contrast between the signal mean pixel value and the background. Figure 2(a) shows that higher frame rates result in a reduction in the background MV noise and a larger contrast between signal and noise. This effect is larger for higher exposures with the difference in the mean pixel values of the signal to background noise being greater at these higher exposures; however small differences between the signal and background mean pixel values the ratio between these two values is small and the SNR equation is considered valid. As the ratio between the background and signal pixel values increases the sensitivity of this equation to change is altered, as seen between 1 Hz to 5 Hz where the change is sharp and the background noise of 1 Hz is five times greater than at 5 Hz.

Figures 2(c) and (d) define the linear effect of the kV to MV ratio with frame rate and exposure, the independent nature of the measurements ignore the limitations of the SNR equation however don't account for kV scatter and visibility. The increase in exposure is shown to improve image quality by a greater percentage than a proportional increase in frame rate. The increase in exposure resulted in a 35.5% and 29.5% improvement in kV to MV ratio and SNR over frame rate respectively. The mean (range) uncertainty, coefficient of variation, in the measurements of SNR was 0.7% (0.4–1.9%) and of kV to MV ratio was 0.7% (0.3–1.0%).

3.3. Effect of patient size on kV parameters required for segmentation

Figure 3(a) shows the effect of patient size on kV mean pixel value. AP and PA kV projections show that as patient size increases the kV signal incident on the detector is reduced. The mean pixel value in the PA and AP projection angles decreases exponentially with increasing patient thickness, while lateral kV fields are unaffected as expected since the phantom dimensions are unaltered in this direction.

Figure 3(b) shows how increasing patient size impacts the amount of MV scatter that is incident on the kV detector. The MV scatter for in AP kV images are shown to remain constant with an increase of thickness on the anterior surface. For the posterior kV projection, where the kV detector is located above the patient, a significant decrease in the MV scatter is detected as the depth of attenuation material is increased. A small increase in MV scatter with patient thickness is shown to occur when the kV detector is located on the lateral side; this is due to the increased scattering through the patient increasing the amount of MV scatter detected. The difference in MLC field shape is shown when 10 cm of water-equivalent material is added to the anterior surface to equal the lateral thickness; more MV scatter is incident on the detector for the AP kV projection angle.

Figures 3(c) and (d) shows the effect of patient size on kV to MV ratio and SNR, where the kV attenuation through a larger patient size is shown to have a large impact on the image quality. Additional thickness placed onto the anterior surface causes a larger kV to MV ratio and SNR when the kV detector is in the PA kV projection angle due to less MV scatter incident on the detector compared to the AP kV projection angle. With small changes in the background mean pixel value the sensitivity of the SNR equation to change is small as shown in figure 2(b) where across constant frame rates the relationship is linear. The error in measurement was <1% for all readings.

3.4. MV dose rate

The effect of MV patient scatter rate (stemming from treatment dose rate) on the image quality is shown in figure 4. As the MV scatter increases with dose rate a reduction in the kV to MV ratio is observed due to the MV signal increasing while the kV signal remains constant. This increase in MV scatter creates an inverse function with dose rate and a linear increase in the MV scatter on the kVD with dose rate. An apparent angular dependence is shown with AP beam showing higher kV to MV ratio than the lateral beam, which stems from the elliptical shape of the phantom used, where the for AP projection the kV beam penetrates less tissue than the MV beam (90° apart).

3.5. Modelling of MV signal and kV signal onto the kV detector

Using the mean pixel values and data acquired in figures 3(a) and (b) a model is fitted to the data of the kV signal and MV signal using the method described in section 2.1.2 Image quality determination figure 5 compares the measured kV to MV ratio to the kV to MV ratio determined using the model, good agreement is shown between the model and the measured kV to MV ratio. The kV linear attenuation co-efficient and the constant is determined to be 0.1606 cm^{-1} for 125 kVp and 1.36 × 106 respectively, where the linear co-efficient can be altered for different kVp to represent the range of energies available. The primary MV linear co-efficient is determined to be 0.0695 cm^{-1} from the data where the literature values predict a range of 0.04942 cm^{-1}–0.05754 cm^{-1} using a mean energy of 1.5–2 MeV and the x-ray attenuation coefficients of water at these energies from NIST Table [11]. The linear attenuation coefficient for the MV scatter was determined to be 0.0999 cm^{-1} from the data acquired where the literature values predict a value of 0.137 cm^{-1} using 0.2 MeV as the mean energy value of patient-scattered radiation at an angle of 90° and using the x-ray attenuation coefficient of water at this energy from NIST Table [11, 12]. A constant value of 4.01×10^4 was determined from the data. Using the literature values for the model determined from the NIST Table [11] the model was shown to predict higher kV to MV ratio relative to the measured kV to MV ratio.

4. **Discussion**

Image quality and its effect on fiducial marker tracking for KIM determined position of the prostate during delivery of standard VMAT treatments was investigated. KIM-guided gated prostate VMAT treatments have now started and the results presented are applied. (Keall et al 2015) Ng et al (Ng et al 2012) previously demonstrated the effectiveness of KIM in monitoring prostate motion during treatment, and its geometric accuracy was demonstrated. However, a high frame rate (typically 10 Hz) was necessary because of reduced image quality due to MV scatter accumulating between image acquisitions. This higher frame rate results in larger imaging doses as reported in Crocker et al (Crocker et al 2012) that have been described for specific current-time product, frame rate and treatment duration. The dose was shown to scale linearly with each of these parameters. Therefore, the dose for arbitrary mAs settings, frame rates and treatment times may be calculated simply (Crocker et al 2012). Reduction in the imaging frame rate and exposure while maintaining adequate fiducial marker segmentation rates could reduce imaging dose and has been investigated in this study.

In this study, with the segmentation code (Poulsen et al 2009, Fledelius et al 2011) used, we demonstrated that for successful fiducial marker segmentation of the fiducials implanted in a Rando phantom the frame rate must be 3 Hz or greater. Relating the image quality at this frame rate to the homogeneous CIRS phantom a kV to MV ratio of 0.16 and a SNR of 1.67 or greater is required for fiducial marker segmentation. This frame rate

corresponds to a respective 70% reduction in dose from using the reference kV parameters. Knowledge of this relationship for segmentation allows for a potential relaxation of imaging parameters and a respective reduction in dose while maintaining accurate fiducial marker registration for smaller patients. It was determined that in order to maintain sufficient image quality for accurate fiducial marker segmentation a halving of the exposure is required for every 4 cm reduction of thickness the kV beam is attenuated through over a patient size of 36.4 cm in the maximum dimension. Similarly, a halving of the frame rate is required with each 2.5 cm reduction in patient size.

A similar relationship was shown with the kV to MV ratio where a halving of the exposure and a halving of the frame rate are required every 4.5 cm and 3 cm reduction in patient size, respectively. This provides an accurate estimate for reducing dose to patients while maintaining image quality and compensating for the range of patient sizes present. The patients with smaller dimensions will have less kV attenuation and higher image quality where 3 Hz allowed for segmentation of the Rando phantom with a maximum patient dimension of 36.4 cm. The imaging dose could be reduced even further with smaller patient's dimensions, with knowledge of the limitations of segmentation stated above where a kV exposure of 0.5 mAs could be used for patients with a maximum dimension below 32 cm. The frame rate of 5 Hz is chosen as a conservative value over the minimum frame rate of 3 Hz, due to uncertainties in segmentation in heterogeneous tissue. This study has informed the patient eligibility criteria, regarding patient size and imaging parameter relationships, for a clinical trial of KIM for gated prostate VMAT (NCT01742403) that specifies 10 Hz only and a patient dimension less than 40 cm, to ensure that image quality will be retained for all patients in the trial and allow for accurate fiducial marker segmentation.

Rose (Rose 1948, Burgess 1999) states that the SNR should be greater than a value of 5 for a 100% probability to identify a target from an environment of white noise with a mean of zero. We show accurate segmentation of the fiducial markers with SNR values lower than 5. The contrast limitation of the Rose SNR equation was evident from large changes in the background & kV signal which are shown to alter the sensitivity of the equation. This study has shown that an increase in the exposure will have a greater effect on image quality than a similar increase in the frame rate. Doubling of the frame rate improved the kV to MV ratio and the SNR by $84.5\% \pm 16.8$ and $50.6\% \pm 13.1$ respectively, where a similar increase of the exposure resulted in an increase of $132.9\% \pm 20.4$ and $101.3\% \pm 4.6$ for the kV to MV ratio and the SNR respectively. This could be used to improve the image quality without increasing dose to the patient and it is recommended that the current kV parameters be changed from 10 Hz at 1mAs to 5 Hz at 2 mAs to take advantage of this improvement in image quality. Image acquisition settings are independent of the gantry angle, which means that a higher-than-necessary image quality occurs during the AP imaging directions to ensure sufficient signal-to-noise ratio to detect the fiducial markers in the lateral projections (Ng et al 2012). With the results obtained in this study it would be possible to use the CT analogy of automatic brightness control to vary the kV parameters with angle and reduce the imaging dose during treatment. VMAT delivery will usually contain variable dose rates and our data will allow for consideration of dose rate on the image quality with KIM.

With knowledge of the patient dimensions, MV dose rate and field size this study can be used to retain image quality with alteration of the frame rate and exposure. This allows for patient specific kV parameters for individual patients and plans to reduce patient dose while improving image quality and accuracy of fiducial marker segmentation. This method can be reproduced to define limitations on different segmentation codes with image quality for a variety of machines and kV imaging modalities which can be used to improve the image quality and reduce patient dose. A model was fitted to the data and could be included into the segmentation code to predict the expected image quality and probability of accurate fiducial marker segmentation, and if required introduce frame averaging to improve image quality and maintain successful fiducial marker segmentation. This model could also be used before treatment to tailor the kV parameters to individual patient dimensions and reduce imaging dose to the patient.

Improvements to imaging hardware could improve image quality without increase in kV parameter settings or increase in dose to the patient. Specifically, systems that allow adaptive kV settings with gantry angle, collection of image signal only during kV pulse, or application of a background subtraction technique (such as proposed by Ling et al (Ling et al 2011a)) would improve image quality for KIM.

Other methods of improving image quality include the use of software post-processing. Filtering in the temporal domain could be applied to increase the CNR of the fiducial markers, such as the Dolph-Chebyshev filter or Recursive filtering, to improve fiducial marker registration without the need to increase dose to the patient. Real-time segmentation for techniques including KIM require fast calculations to maintain real time stream, incorporation of large imaging processing methods can increase the calculation time and introduce computation lag. The above methods require very little computational power and could be integrated into KIM. Computation power is also continually increasing and higher computational power and methods to enhance current computational power will allow further image enhancement techniques.

5. **Conclusion**

The effect of various kV parameter settings for use during Kilovoltage Intrafraction Monitoring on image quality was assessed and was related to the dose. The image quality depends on x-ray settings, MV beam characteristics, patient thickness and kV detector frame rate. The effect of MV scatter during concurrent treatment was shown to affect image quality and degrades the usability of the image for fiducial marker tracking. It was shown that with alteration of the exposure and frame rate the kV parameters can be tuned to optimal settings, which could be used to improve the image quality and decrease the impact of MV scatter.

The fiducial marker segmentation software was shown to accurately predict the fiducial marker location when the kV to MV ratio and SNR was above 0.16 and 1.67 respectively for 1mAs using the Rando phantom, represented by frame rates above 3 Hz. A previous study showed that the dose to the patient at 10 Hz at 1 mAs was 2 Gy over the course of an 80 Gy in standard VMAT.

Our analysis has indicated that for patient sizes less than 36.4 cm, the optimisation of image quality for fiducial marker tracking could lead to a halving of imaging dose (i.e. from 2 Gy over the course of treatment to 1 Gy). Furthermore, we have shown that by changing the reference parameters to 5 Hz at 2 mAs an increase in the image quality is observed with no effect on the patient dose. A model was produced to predict the expected kV to MV ratio with changing patient size to allow for optimization and reduction of the imaging dose to individual patients.

For the broader application of KIM for use with larger patients, larger MV field sizes and higher dose rates, individualisation of the kV parameters is needed. It has been shown that by tailoring the kV parameters to patient size, image quality can be increased and the flexibility of this method can be used to include a much larger range of patients and treatment types while maintaining acceptable patient dose.

Appendix

Modelling of the MV signal and kV signal onto the kV detector

Modelling of the MV signal onto the kV detector is determined using the following equation from Spies et al (Spies et al 2000). Assuming the beam to be pencil-like and assume further that this beam is monochromatic we

can find a simple expression for the number of single-scattered photons on-axis is proportional to (Spies et al 2000):

$$e^{-\mu L}\int_0^L \frac{d\zeta}{(\zeta+\delta)^2} = e^{-\mu L}\left[\frac{L}{\delta(L+\delta)}\right] \quad (3)$$

where μ is the attenuation coefficient of the phantom for the given beam energy, L denotes the thickness (water-equivalent thickness for our case) of the phantom, δ is the air gap between the detector and the phantom and z is the depth scattered photons are created at. This formulation is used to calculate the MV scatter at the centre of the phantom (also isocentre) from the primary beam and also to calculate the proportion of this scatter reaching the kV detector in our set-up. We define $\delta_{\text{to-iso}}$ as the air gap from the phantom surface to the MV source. The following equations can be used to determine the MV scatter at the kVD.

Equation (4) defines the scatter at the centre of the phantom where $I_{\text{MV(patient-scatter)}}$ is the scatter at the centre of the phantom, $\text{MV}_{\text{Field Size}}$ is the field size of the MV beam, Dose rate is the dose rate, $L_{\text{MV(Primary)}}$is the water-equivalent thickness to the centre of the phantom and $\mu_{\text{MV(Primary)}}$ attenuation coefficient of the primary beam.

$$I_{MV(patient-scatter)} = Constant \times MV_{Field\ Size} \times Dose\ rate \times e^{-\mu_{MV(Primary)} \times L_{MV(Primary)} * \left[\frac{L_{MV(Primary)}}{\delta_{to-iso}(L_{MV(Primary)}+\delta_{to-iso})}\right]} \quad (4)$$

Equation (5) defines the amount of scatter incident on the kVD where $I_{\text{MV(kVD)}}$ is the amount of scatter incident on the kVD, $\mu_{\text{MV(scatter)}}$ is the attenuation coefficient of the scatter radiation, $L_{\text{MV(scatter)}}$ is the water-equivalent thickness from the centre of the phantom to the edge of the phantom in the kVD direction in cm and $\text{kV}_{\text{image interval}}$ is the frame rate of the detector defined in Hz and $\delta_{\text{to-kVD}}$ is the air gap from the edge of the phantom to the kV detector.

$$I_{MV(kVD)} = I_{MV(patient-scatter)} \times kV_{image\ interval} \times e^{-\mu_{MV(scatter)} \times L_{MV(scatter)} * \left[\frac{L_{MV(scatter)}}{\delta_{to-kVD}(L_{MV(scatter)}+\delta_{to-panel})}\right]} \quad (5)$$

The modelling of kV signal onto the detector is determined from the following equation. Where $I_{\text{kVD}}$is the signal incident on the kVD, μ_{kV} is attenuation coefficient of the phantom for the given kV energy, L_{kV} denotes the thickness of the phantom that the kV beam travels through, SDD is the Source to Detector Distance in cm and mAs is the kV exposure.

$$I_{kVD} = \frac{100}{SDD^2} \times Constant \times mAs \times kV_{image\ interval} \times e^{-\mu_{kV} \times L_{kV}} \quad (6)$$

The ratio of equations (5) and (6) can be used to determine the theoretical kV to MV ratio as shown in equation (7).

$$kV\ to\ MV\ Ratio = \frac{I_{kVD}}{I_{MV(kVD)}} \quad (7)$$

References

Adamson J and Wu Q 2009 Optimizing monoscopic kV fluoro acquisition for prostate intrafraction motion evaluation Phys. Med. Biol. 54 117

Burgess A E 1999 The Rose model, revisited J. Opt. Soc. Am. A 16 633–46

Colvill E, Poulsen P R, Booth J, O'Brien R, Ng J and Keall P 2014 DMLC tracking and gating can improve dose coverage for prostate VMAT Med. Phys. 41 091705

Crocker J K, Ng J A, Keall P J and Booth J T 2012 Measurement of patient imaging dose for real-time kilovoltage x-ray intrafraction tumour position monitoring in prostate patients Phys. Med. Biol. 57 2969

Fledelius W, Worm E, Elstrom U V, Petersen J B, Grau C, Hoyer M and Poulsen P R 2011 Robust automatic segmentation of multiple implanted cylindrical gold fiducial markers in cone-beam CT projections Med. Phys. 38 6351–61

Keall P J, Ng J A, O'Brien R, Colvill E, Huang C-Y, Poulsen P R, Fledelius W, Juneja P, Simpson E and Bell L 2015 The first clinical treatment with kilovoltage intrafraction monitoring (KIM): a realtime image guidance method Med. Phys. 42 354–8

Ling C, Zhang P, Etmektzoglou T, Star-Lack J, Sun M, Shapiro E and Hunt M 2011a Acquisition of MV-scatter-free kilovoltage CBCT images during RapidArc or VMAT Radiother. Oncol. 100 145–9

Ling C, Zhang P, Etmektzoglou T, Star-lack J, Sun M, Shapiro E and Hunt M 2011b Acquisition of MV-scatter-free kilovoltage CBCT images during RapidArc™ or VMAT Radiother. Oncol. 100 145–9

Lovelock D M, Messineo A P, Cox B W, Kollmeier M A and Zelefsky M J 2015 Continuous monitoring and intrafraction target position correction during treatment improves target coverage for patients undergoing sbrt prostate therapy Int. J. Radiat. Oncol. Biol. Phys. 91 588–94

Luo W, Yoo S, Wu Q, Wang Z and Yin F-F 2008 Analysis of image quality for real-time target tracking using simultaneous kV–MV imaging Med. Phys. 35 5501–9

Maria Aresu G B and Bryson A 2010 Health Survey for England—2010, Respiratory Health (London: Health and Social Care Information Centre) HSE: vol 10

Morris L, Stevens M J, Valmadre S, Martland J and Lee T 2012 Adjuvant intravaginal brachytherapy for uterus didelphys with synchronous endometrial adenocarcinomas and unfavourable vaginal topography Gynecol. Oncol. Rep. 2 121–3

Ng J A, Booth J T, Poulsen P R, Fledelius W, Worm E S, Eade T, Hegi F, Kneebone A, Kuncic Z and Keall P J 2012 Kilovoltage intrafraction monitoring for prostate intensity modulated arc therapy: first clinical results Int. J. Radiat. Oncol. Biol. Phys. 84 e655–61

Poulsen P R, Cho B and Keall P J 2009 Real-time prostate trajectory estimation with a single imager in arc radiotherapy: a simulation study Phys. Med. Biol. 54 4019

Poulsen P R, Cho B, Langen K, Kupelian P and Keall P J 2008 3D prostate position estimation with a single x-ray imager utilizing the spatial probability density Phys. Med. Biol. 53 4331

Rose A 1948 The sensitivity performance of the human eye on an absolute scale J. Opt. Soc. Am. 38 196–208

Sandler H M, Liu P-Y, Dunn R L, Khan D C, Tropper S E, Sanda M G and Mantz C A 2010 Reduction in patient-reported acute morbidity in prostate cancer patients treated with 81Gy intensity-modulated radiotherapy using reduced planning target volume margins and electromagnetic tracking: assessing the impact of margin reduction study Urology 75 1004–8

Seibert J A 2004 Tradeoffs between image quality and dose Pediatr. Radiol. 34 S183–95

Spies L, Evans P M, Partridge M, Hansen V N and Bortfeld T 2000 Direct measurement and analytical modeling of scatter in portal imaging Med. Phys. 27 462–71

van Herk M, Ploeger L and Sonke J-J 2011 A novel method for megavoltage scatter correction in conebeam CT acquired concurrent with rotational irradiation Radiother. Oncol. 100 365–9

Table 1. Effect of frame rate on the segmentation success and its relationship to kV to MV ratio and SNR as defined in equations (1) and (2).

Frame Rate (Hz)	Segmentation	kV to MV ratio	SNR
1	No	0.08	1.11
2	No	0.11	1.33
3	Yes	0.16	1.67
4	Yes	0.20	2.01
5	Yes	0.24	2.42
10	Yes	0.45	3.63
15	Yes	0.64	4.55

Figure 1. Photograph of experimental setup with the CIRS phantom with added water-equivalent material to enable the investigation of different phantom sizes.

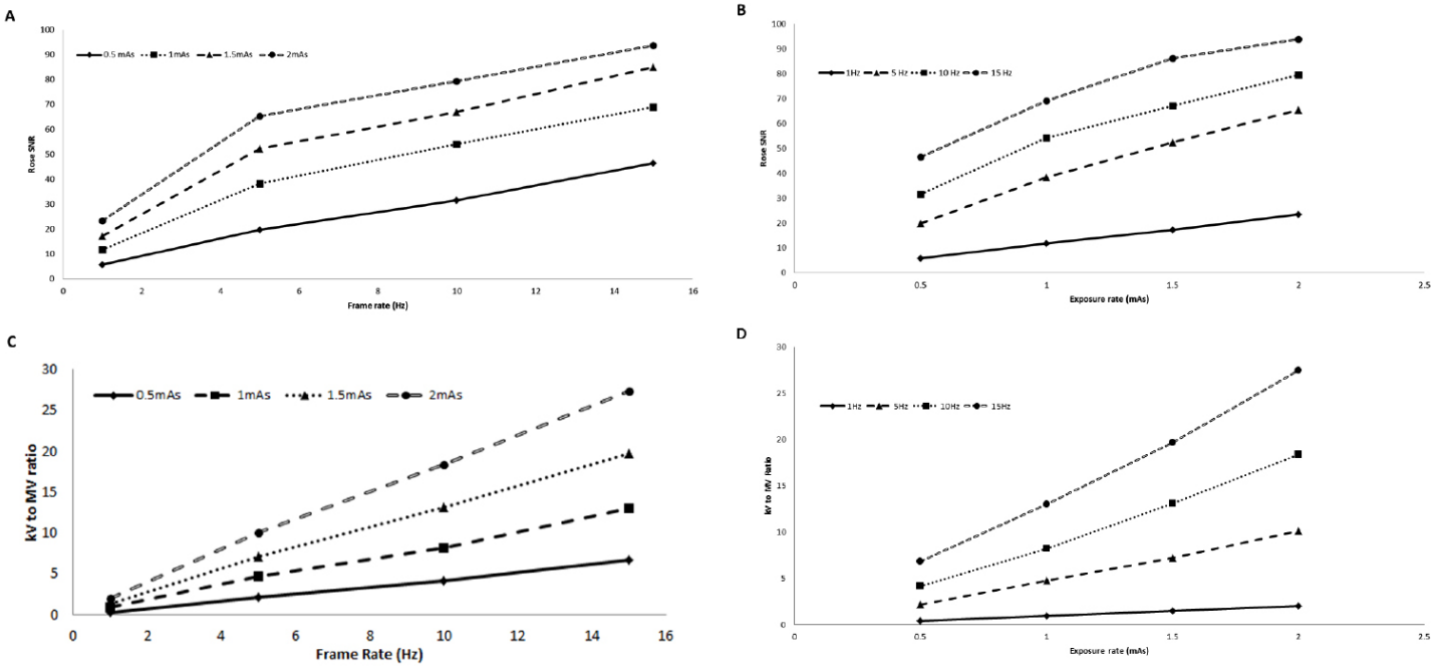

Figure 2. Relationship between SNR and (a) image panel frame rate and (b) kV exposure; and image quality (kV to MV ratio) and (c) image panel frame rate and (d) kV exposure. The projection angle is 0°.

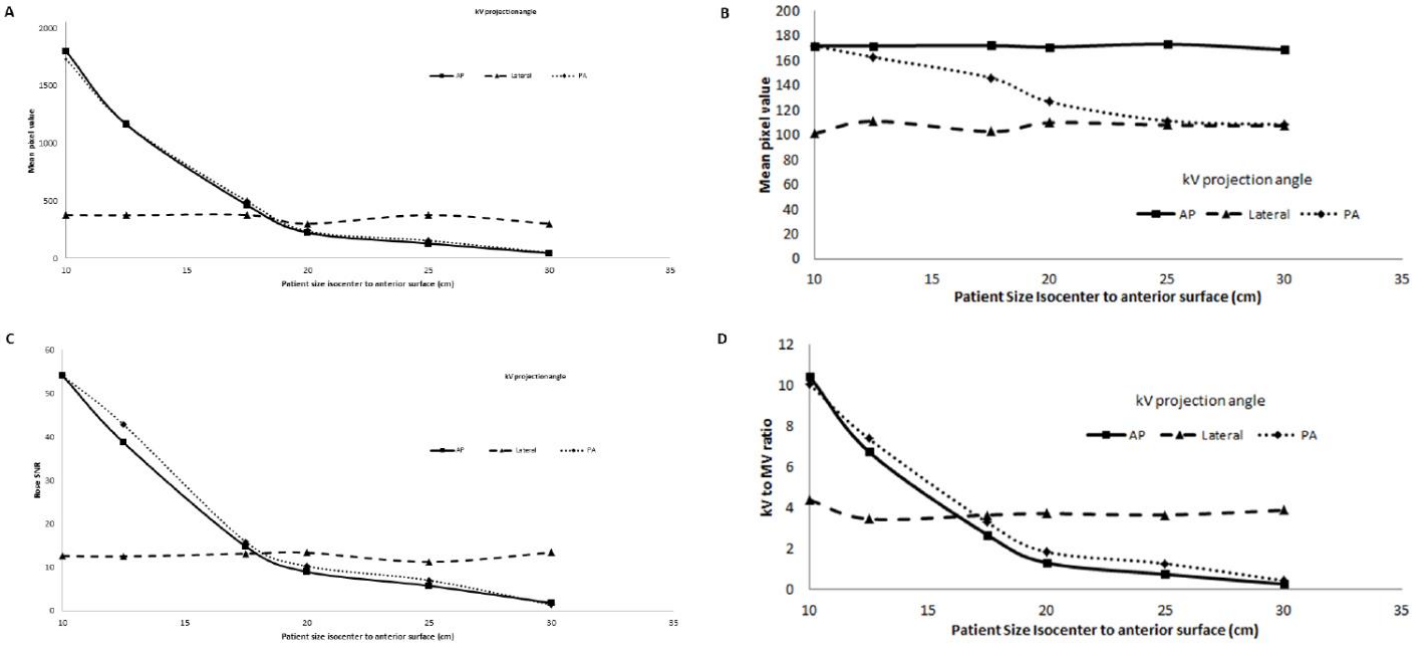

Figure 3. Relationship between patient size and kV image quality surrogate for baseline kV parameters (a) transmitted kV signal alone (mean pixel value) (b) MV beam scattered to kV detector panel (c) signal to noise ratio, and (d) ratio of pixel values shown is (a) and (b) as the kV to MV ratio.

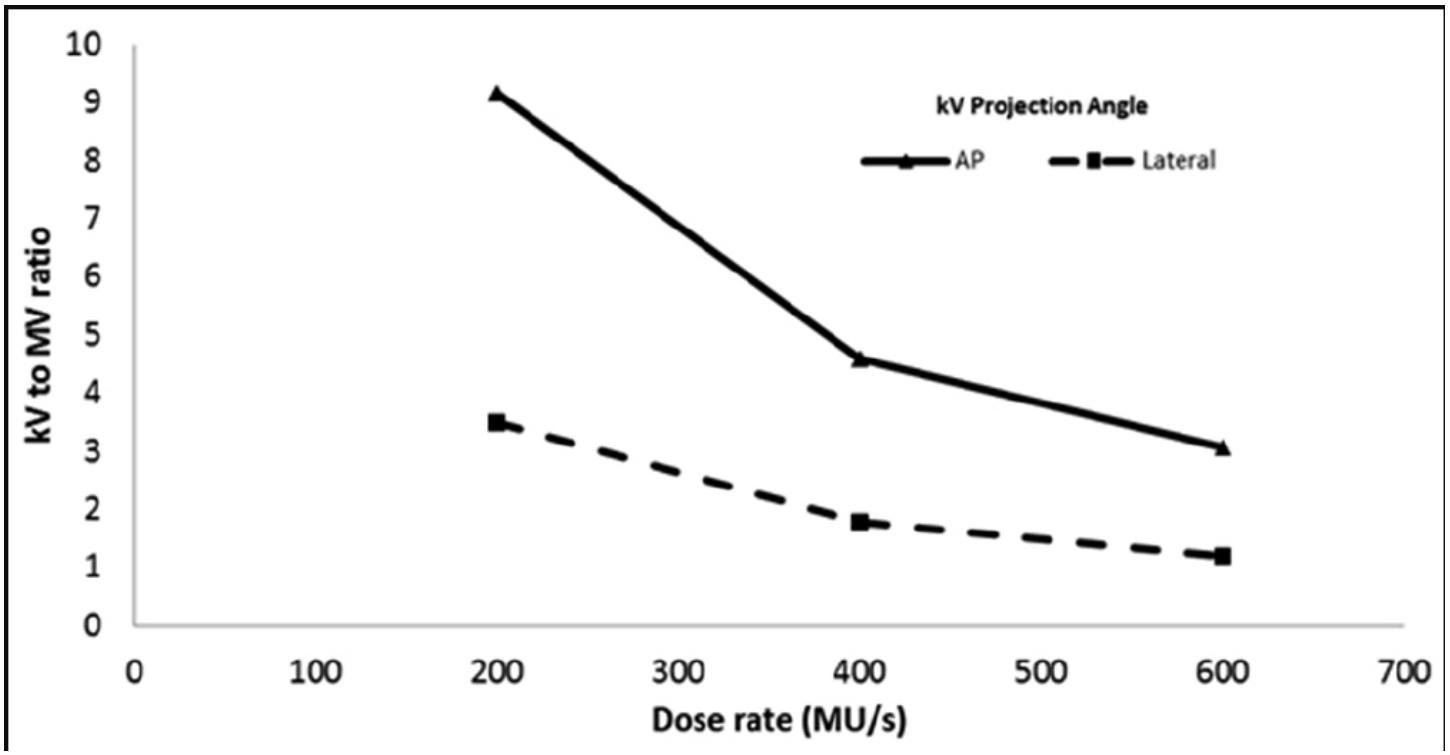

Figure 4. The effect of MV dose rate on the kV to MV ratio.

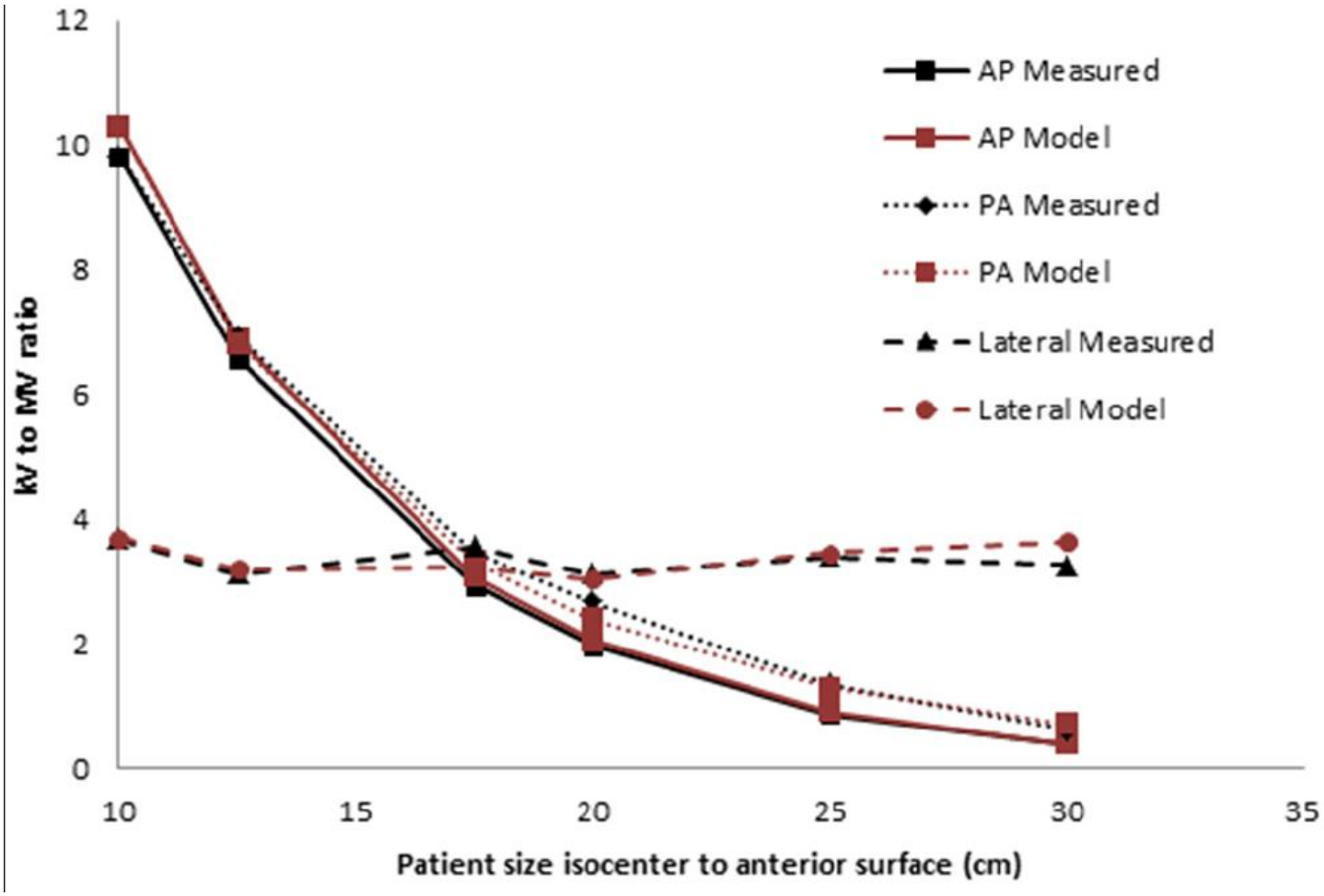

Figure 5. Effect of patient size on kV to MV ratio comparing measured (solid) and calculated (dashed) values.